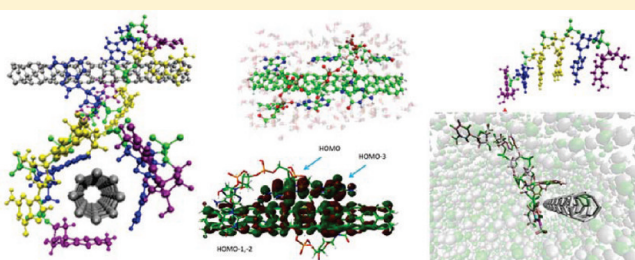


DNA–CNT Interactions and Gating Mechanism Using MD and DFT

Alfredo D. Bobadilla^{†,‡} and Jorge M. Seminario^{*,†,‡,§}

[†]Department of Chemical Engineering [‡]Department of Electrical and Computer Engineering [§]Materials Science and Engineering Graduate Program, Texas A&M University College Station, Texas 77843, United States

ABSTRACT: DNA molecules are able to wrap carbon nanotubes (CNTs) in water solution, thus merging advantages of DNA chemistry with CNT physics as a natural way to design sensor devices. Using electrical means, a reversible semiconductor–metallic behavior has been found in CNT–DNA hybrid structures. Classical molecular dynamics simulations of the CNT–DNA wrapping process are performed. Then, structural conformations are analyzed by first-principles electronic structure methods; we correlate our results with previous experimental reports on carbon–DNA complexes, providing complementary information to understand better their electrical behavior.



■ INTRODUCTION

Diverse efforts have been performed on carbon nanotube (CNT)^{1–4} and DNA-based nanoelectronic devices^{5–9} because both show potential as fundamental elements for molecular electronics.^{10–16} The combination of the chemical sensing capabilities of DNA and the electrical properties of CNT in a hybrid nanodevice has been proposed for very sensitive detection of chemical events at the single-molecule level^{17,18} and a molecular understanding of CNT–DNA interaction can yield new insights to develop devices for rapid DNA sequencing^{19,20} as well as to improve the development of nanosensors, especially for chemical and biological agents.^{5,8,21–28}

Gowtham et al.²⁹ studied the physisorption of individual nucleobases on graphene using DFT methods, finding significant differences between interaction strengths when a nucleobase is physisorbed on graphene; based on an analysis of binding energies, they suggested that the base molecule polarizabilities are the main factors determining the nucleobase–graphene interaction strength. In another study by the same authors, the strength of the interaction was analyzed between DNA bases and a small diameter carbon nanotube of chirality (5,0).³⁰ It is known that π – π interaction is the main factor driving single-stranded DNA (ssDNA) wrapping around large diameter carbon nanotube.³¹ Nevertheless, the high curvature surface in a small diameter nanotube implies a nonplanar hexagonal geometry, which would decrease π – π stacking interaction. Analyzing this kind of interaction, Gowtham et al.³⁰ found a correlation between nucleobases polarizability and CNT–nucleobase binding energies which resulted to follow the hierarchy G > A > T > C > U, concluding that molecular polarizability of nucleobases plays the dominant role in the interaction strength of nucleobases with CNT.³⁰

It has been reported that a DNA wrapped carbon nanotube device can change from metallic behavior in dry conditions to semiconductor behavior in wet conditions.³² Ouellette et al.³³

analyzed the time evolution of electrical current in a suspended carbon nanotube positioned in a microfluidic channel through which DNA molecules were allowed to flow. They observed the appearance of spikes when DNA molecules were present in the microfluidic channel; DNA molecules constantly flowed through the microfluidic channel and electrostatic screening of van der Waals interaction due to ions was minimized.

In the present work, structural conformations and electronic structure of CNT–DNA hybrids are analyzed with molecular dynamics and first-principles quantum chemistry techniques searching for further insights on the mechanisms responsible for semiconductor–metallic behavior in DNA wrapped carbon nanotube.

2. METHODOLOGY

The Large-scale Atomic/Molecular Massively Parallel Simulator (LAMMPS)³⁴ program is used to perform molecular dynamics simulations of solvated CNT–DNA. The chosen single-stranded DNA sequence is TAGGAT and the single-walled carbon nanotube is a zigzag (4,0). Ions are added to the water solution to neutralize the negative charge in DNA backbone due to negatively charged phosphate groups thus yielding a neutral whole system. The solution contains 11 Na⁺, 6 Cl⁻, and 1,869 TIP3P^{35,36} water molecules in a simulation box of 40 × 40 × 40 Å³. The initial atomic coordinate file is generated with the Packing Optimization for Molecular Dynamics Simulations (*Packmol*).³⁷ Periodic boundary conditions are applied to the box and run under the microcanonical NVE ensemble. Electrostatic interactions are calculated by the particle–particle and particle–mesh (PPPM)³⁸ method using a grid order of 4.

Received: October 23, 2010

Revised: December 27, 2010

Published: February 07, 2011

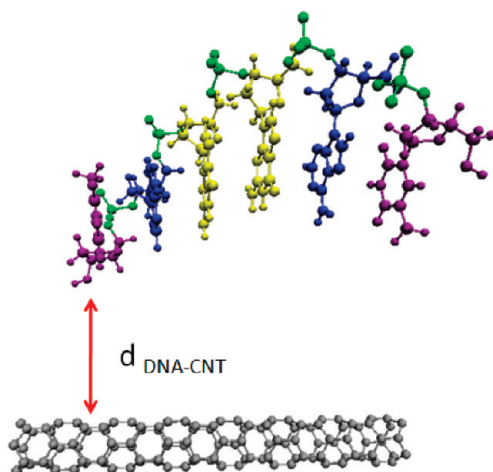


Figure 1. Initial conformation for molecular dynamics simulation of solvated CNT–DNA, CNT chirality is (4,0). Water molecules (density = 1 g/cm³) and counterions have been removed for the sake of visualization. DNA molecule is color coded: thymine (violet), adenine (blue), guanine (yellow), phosphate groups (green). $d_{\text{DNA-CNT}} = 11.5$ Å is the distance between the thymine base and the carbon nanotube.

Table 1. Lennard–Jones and Coulombic Interactions Are Computed with an Additional Switching Function $S(r)$ Detailed in eq 3

cutoff	Lennard–Jones	coulombic
$r < r_{\text{in}}$	$V_{\text{LJ}}(r)$	$C(r)$
$r_{\text{in}} < r < r_{\text{out}}$	$S(r) \times V_{\text{LJ}}(r)$	$S(r) \times C(r)$
$r > r_{\text{out}}$	0	0

To control the temperature, within the NVE ensemble, atom velocities are rescaled at every time-step with the Berendsen thermostat,³⁹ which is applied to only the translational degrees of freedom. The positions of all CNT atoms are constrained by not updating the velocity for atoms in the CNT as expected applications consider the CNT fixed to metal electrodes.

In the initial conformation for the molecular system, the closest distance between ssDNA and CNT is 11.5 Å (Figure 1). An energy minimization of the system is performed to reach a local potential energy minimum. Then, the temperature of the system is raised from 5 to 300 K in a 0.525 ns run. This is followed by a 1.05 ns run at 300 K to ensure equilibration. To accelerate the wrapping process the temperature is raised to 340 K in a 1.05 ns MD run, then the system is allowed to equilibrate at 340 K for 7.5 ns. Visualization of trajectories is performed using the graphics software package VMD.⁴⁰

To model the system, the CHARMM force field⁴¹ is used, in which the van der Waals energy is calculated with a standard 12–6 Lennard–Jones potential,

$$V_{\text{LJ}}(r) = 4\epsilon \left[\left(\frac{\sigma}{r} \right)^{12} - \left(\frac{\sigma}{r} \right)^6 \right] \quad (1)$$

modeling nonbonded interactions between pairs of atoms at distance r , separated by at least three consecutive bonds. It is composed of two terms: the first describes the Pauli repulsive interaction at short ranges due to overlapping electron orbitals and the second describes the van der Waals attractive interactions, which at long ranges are due to dipole–dipole interactions

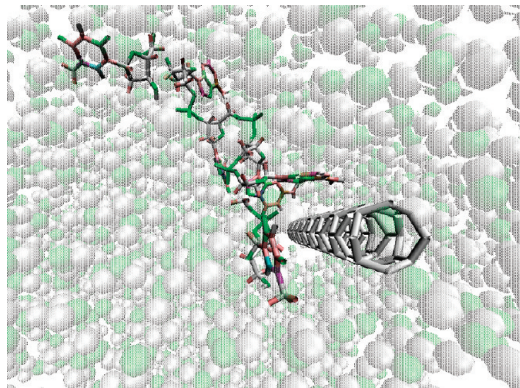


Figure 2. Snapshot at $t = 2.6$ ns: DNA molecule approaching CNT at the initial stage of the process at 340 K. The high temperature accelerates the van der Waals attraction between DNA bases and the carbon nanotube surface.

and to the fluctuating molecular dipole moments. ϵ is the Lennard–Jones well depth and σ is the distance at the Lennard–Jones minimum.

The electrostatic energy with a coulombic potential,

$$C(r) = \frac{1}{4\pi\epsilon} \frac{q_i q_j}{r_{ij}} \quad (2)$$

represents interactions between static atomic charges q_i and q_j at distance r_{ij} , and ϵ is the dielectric constant.

The coefficients σ and ϵ are defined for each pair of atoms according to the CHARMM force field. The Lennard–Jones parameters between pairs of different atoms are obtained from the Lorentz–Berthelot combination rules, in which ϵ_{ij} values are based on the geometric mean of ϵ_i and ϵ_j and σ_{ij} values are based on the arithmetic mean between σ_i and σ_j . Both Lennard–Jones and coulombic interactions are computed with an additional switching function $S(r)$,³⁶

$$S(r) = \frac{[r_{\text{out}}^2 - r^2]^2}{[r_{\text{out}}^2 - r_{\text{in}}^2]^3} [[r_{\text{out}}^2 + r^2 - 3r_{\text{in}}^2]] \quad (3)$$

which decreases the interaction energies smoothly to zero from an inner (r_{in}) cutoff to an external cutoff (r_{out}), in order to decrease the number of hot spots in the simulation. We use, $r_{\text{in}} = 8$ Å and $r_{\text{out}} = 10$ Å, for both, Lenard–Jones and coulombic non-bonded interactions (Table 1). CNTs are modeled as uncharged Lennard–Jones particles using sp² carbon parameters from the CHARMM force field.

3. RESULTS AND DISCUSSION

At the initial stage of the process at 340 K, the DNA molecule approaches the carbon nanotube as shown in Figure 2. During the first 2.5 ns of the equilibration process at 340 K, the DNA molecule stay noncovalently linked to the carbon nanotube and only two or three bases participate in the CNT–DNA interaction. From 2.5 to 5 ns, the DNA molecule wraps the carbon nanotube forming a circle around the nanotube (parts a and b of Figure 3). At the end of the process at 340 K, from 5 to 7.5 ns, the DNA molecule changes its structural conformation forming a helical wrapping around the nanotube (parts c and d of Figure 3), and 5 bases, out of 6, are oriented parallel to the CNT. Nevertheless,

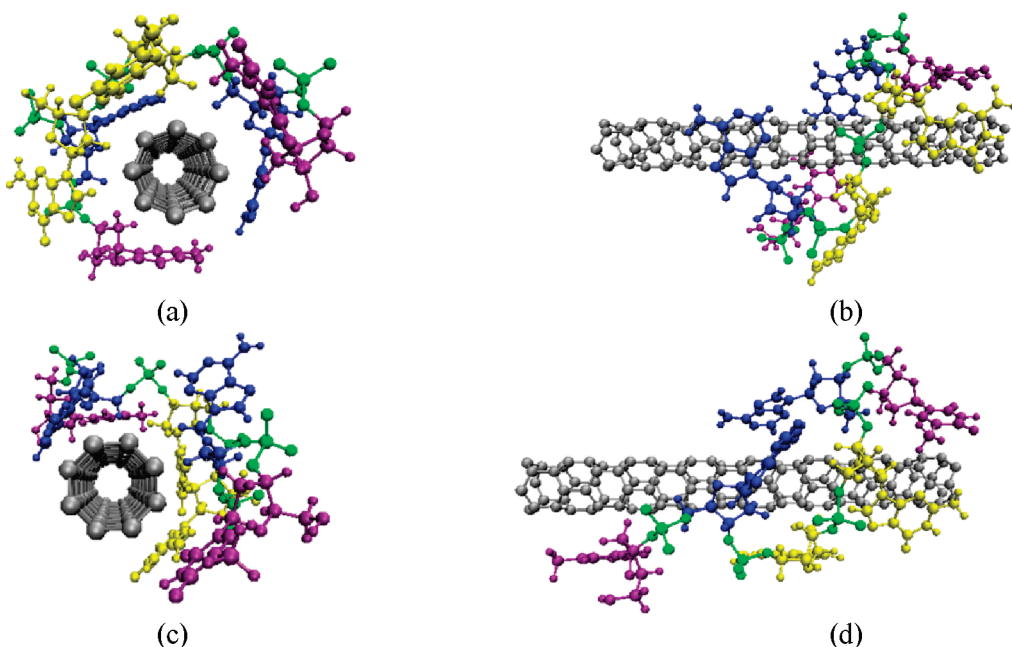


Figure 3. (a) Front and (b) side view of DNA–CNT circular wrapping after 6.4 ns, at the middle stage of the process at 340 K. (c) Front and (d) side views of the DNA–CNT helical wrapping after 10.1 ns, at the final stage of the process at 340 K (color code as in Figure 1).

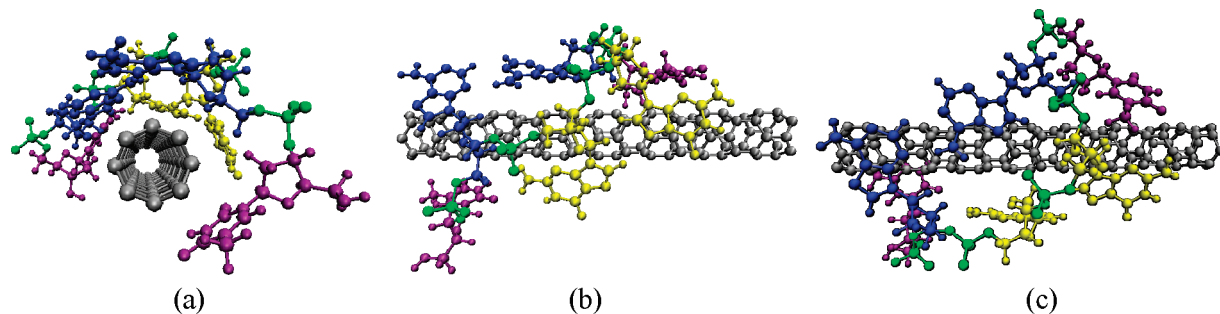


Figure 4. (a) Front view of DNA–CNT helical wrapping after 12.2 ns, at the final stage of equilibration at 300 K. (b) and (c) show two side views (color code as in Figure 1).

in the following process from 340 to 300 K all bases prefer an orientation parallel to the carbon nanotube, keeping that tendency during the final equilibration at 300 K (Figure 4). The system is considered to be in equilibrium when the root-mean-square deviation (rmsd), calculated for DNA structure with respect to its initial conformation, keeps a constant value.

We calculate the van der Waals (vdW) energy (part b of Figure 5) between DNA molecule and single-walled carbon nanotube; the time evolution of this energy shows significant energy jumps (part b of Figure 5) occurring due to absorption of DNA bases on the carbon nanotube surface. The electrostatic energy of interaction between adjacent phosphate atoms is shown in part c of Figure 5. During the first 2 ns of equilibration process at 340 K, the ssDNA adopts a conformational structure in which the phosphate atoms are closer between them; this causes an increase of their electrostatic energy. Then, as ssDNA conformational changes around CNT progress, a decrease in electrostatic energy corresponding to an increase in distance between phosphate atoms when ssDNA adopts a helical conformation around CNT.

The final structural conformation shows that each base type prefers a particular orientation with respect to the DNA backbone;

the two thymine bases and the two guanine bases prefer an orientation opposite to that preferred by the two adenine bases. The ssDNA form a right-handed helical wrapping around the carbon nanotube.

After the ssDNA is physisorbed on the carbon nanotube (CNT) surface, the DNA experiences free translational and angular movements along the CNT surface, persisting through the equilibration process at room temperature.

The self-assembly of carbon nanotube and DNA is usually driven mainly by $\pi-\pi$ stacking interactions, enabled by the planar hexagonal conjugated π -systems in single-walled CNT. However, in a CNT (4,0), the carbon skeleton forms boatlike nonplanar hexagonal conjugates (Figure 6) due to the high curvature surface in small diameter nanotubes; we expected this to be an obstacle for $\pi-\pi$ stacking interactions. Despite of the large strain energy imposed on the CNT (4,0), ab initio molecular orbital calculations at the B3PW91/6-31G(d) level still show a large delocalization of a benzene strained to the same curvature that it would have in the small CNT(4,0). Figure 7 shows a comparison of the relevant molecular orbitals of the two benzene conformations. The injection of a small sp^3 contribution with a dangling bond might increase the interaction with any part

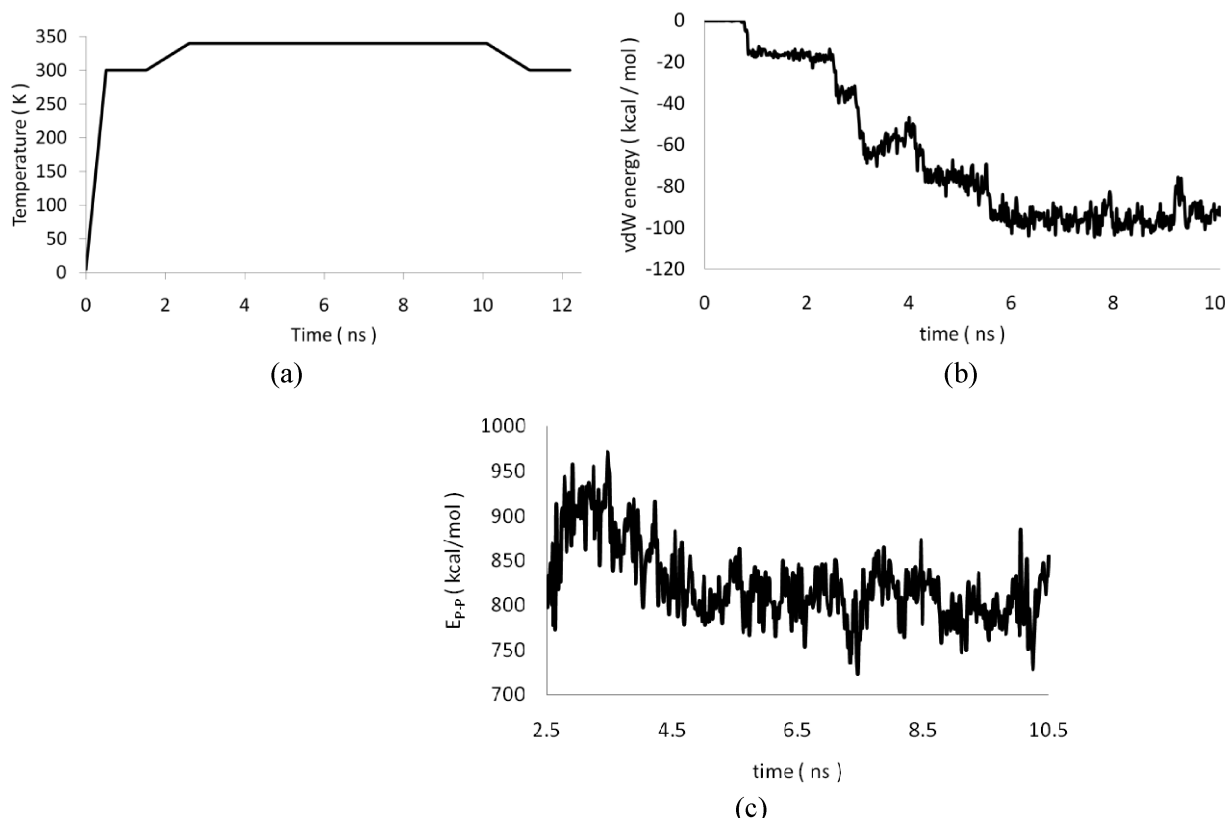


Figure 5. (a) Input temperature temperatures: the equilibration process at 340 K begins at $t = 2.6$ ns and finishes at $t = 10.1$ ns. (b) Energy jumps are observed in van der Waals (vdW) energy as each nucleotide base binds to the carbon nanotube surface. (c) Electrostatic energy of phosphate atoms in the ssDNA backbone during equilibration process at 340 K.

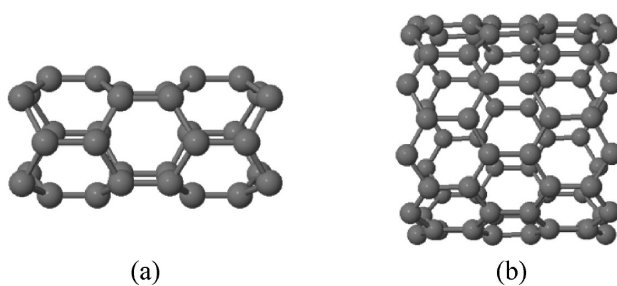


Figure 6. (a) Boatlike nonplanar hexagonal conjugates in CNT(4,0) and (b) planar hexagonal conjugated π -systems in CNT(10,0).

of the DNA and not only with its π regions. There is still certain similarity between the molecular orbitals of the two conformations but energies of the frontier molecular orbitals are strongly affected decreasing the effect away from the frontier orbitals.

To analyze the electronic band structure, ab initio electronic structure calculations are performed in vacuum and aqueous conditions at the B3LYP/6-31G(d) level for the carbon nanotube, DNA molecule and DNA-wrapped carbon nanotube system.

To simulate aqueous conditions with low computational cost, the Tomasi's polarizable continuum model (PCM)⁴² is used; in this method, the solvent is modeled as a continuum of uniform dielectric constant. The molecular system is placed into a cavity within the solvent and the calculation of the molecular electrostatic potential or the electric field at a discrete number of preselected points is utilized to evaluate the environmental effects of a solvent on the properties of the molecular system.

For more accurate results, we consider the water molecules surrounding the hybrid structure (part c of Figure 8). We also perform molecular dynamics simulations for individual carbon nanotube (part b of Figure 8) and individual DNA (part a of Figure 8) in water solvent to get the corresponding structural conformation and to analyze differences in electronic structure with respect to the hybrid structure.

As shown in Table 2, our results using the PCM method differ much from those with water molecules surrounding carbon nanotube and DNA. The lack of accuracy of the PCM method arises from considering only electrostatic effects in the interaction between the solvent and the molecular system.

We find slight differences in the density of states for CNT in vacuum and under the PCM solvent (Figure 9); there is a strong difference when the actual water molecules are considered in the calculation as they are able to fill states around the frontier orbitals of the CNT and DNA. To be able to analyze contributions from the carbon nanotube (CNT) and DNA to the DOS of the hybrid structure, we identify the highest occupied molecular orbitals (HOMO) and the lowest unoccupied molecular orbitals (LUMO) for CNT and DNA when they are part of the hybrid structure; this is done by visualizing the molecular orbitals (MO) for each energy state and identifying the molecules on which each MO is localized. These results are summarized in Table 2 and Figure 10.

Comparing individual molecules with the hybrid structure at vacuum conditions (Table 3), we observe that the HOMO and LUMO orbitals corresponding to the carbon nanotube are almost unaffected by the wrapping of DNA molecule; however,

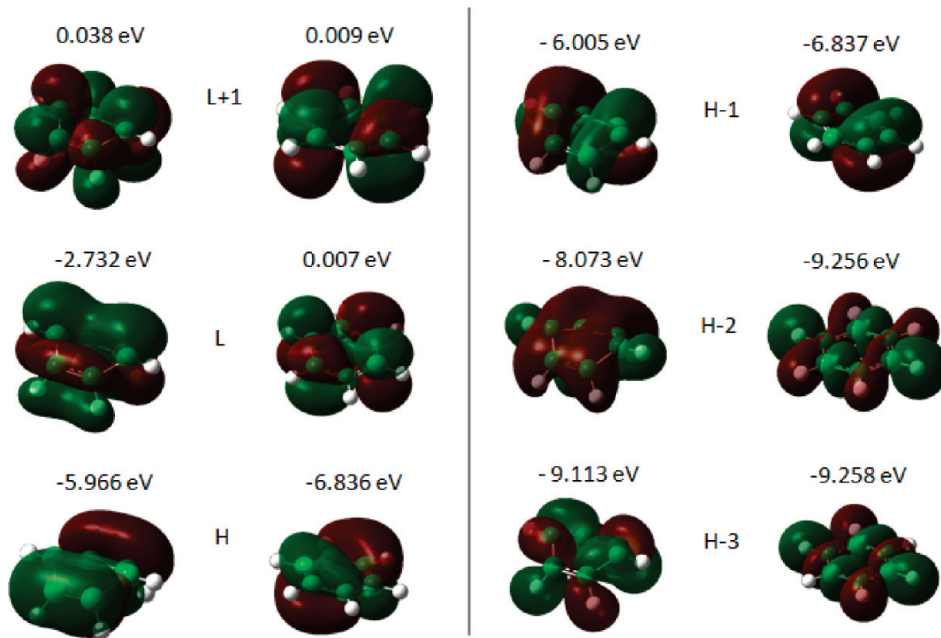


Figure 7. Comparison of molecular orbitals (H = HOMO, L = LUMO) and energies for benzene (2nd and 4th columns) and strained benzene with the curvature of a CNT(4,0) (1st and 3rd columns).

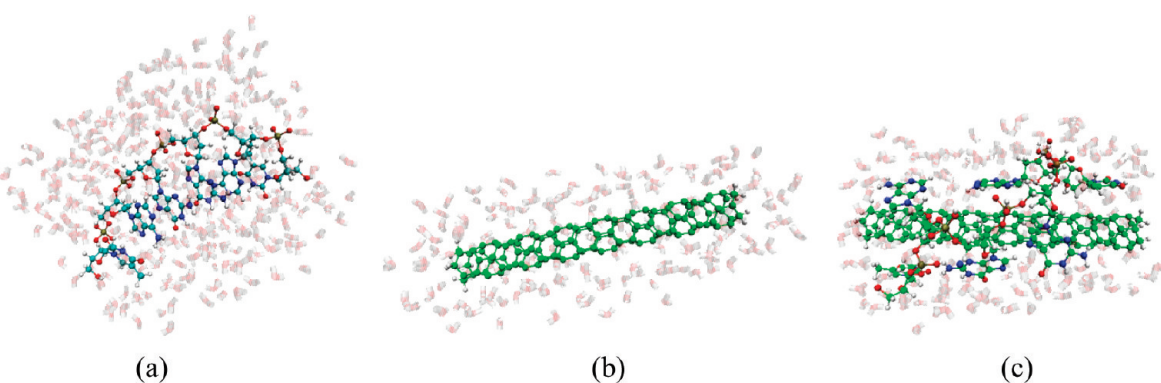


Figure 8. Structural conformations from molecular dynamics simulations for the ab initio calculations performed in water solvent: (a) DNA, (b) carbon nanotube, and (c) CNT–DNA nanostructure.

Table 2. Number of Atoms Involved in the Molecular DFT B3LYP/6-31G(d) Calculations; Length of the CNT(4,0) is 3 nm and the ssDNA Sequence is TAGGAT; Carbon Nanotube and DNA Molecule Are Passivated with Hydrogen Atoms

system	number of atoms	number of water	number of atoms
	in vacuum conditions	molecules in aqueous conditions	in aqueous conditions
CNT	136	172	652
ssDNA	198	334	1200
ssDNA–CNT	334	179	871

we observe that the DNA HOMO orbital shifts to an energy level higher than the energy of the CNT HOMO, producing a hybrid structure energy gap of 0.31 eV smaller than the one of the carbon nanotube. We also observe that the DNA energy gap decreases, enabling an additional path for electron flow. These two factors contribute therefore to a metallic behavior. Electrons may flow not only from metal electrodes to carbon nanotube but

also from metal electrodes to DNA and from DNA to carbon nanotube in a scenario similar to the experiment reported by Cha et al.³² who reported a metallic behavior for the hybrid structure in vacuum conditions; in their experimental setup, it was possible a direct contact between ssDNA and metal electrodes.

The individual carbon nanotube in water conditions shows a less stable behavior than in vacuum conditions, with a significant energy shift of HOMO and LUMO toward higher energy levels (Table 3) due to the known hydrophobic character of a carbon nanotube molecule produced by its highly symmetric and nonpolar electronic structure. However the electronic structure seems slightly harder with water as its hardness increases by 0.03 eV; on the other hand, DNA suffers a strong change to lower hardness when the water molecules are included in the complex or isolated.

There is a ~0.5 eV energy shift in carbon nanotube HOMO and LUMO to lower energy levels from vacuum to water solvent conditions for the hybrid structure. This increase in global stability of DNA wrapped in a carbon nanotube in water is due to the highly hydrophilic character of phosphate groups located

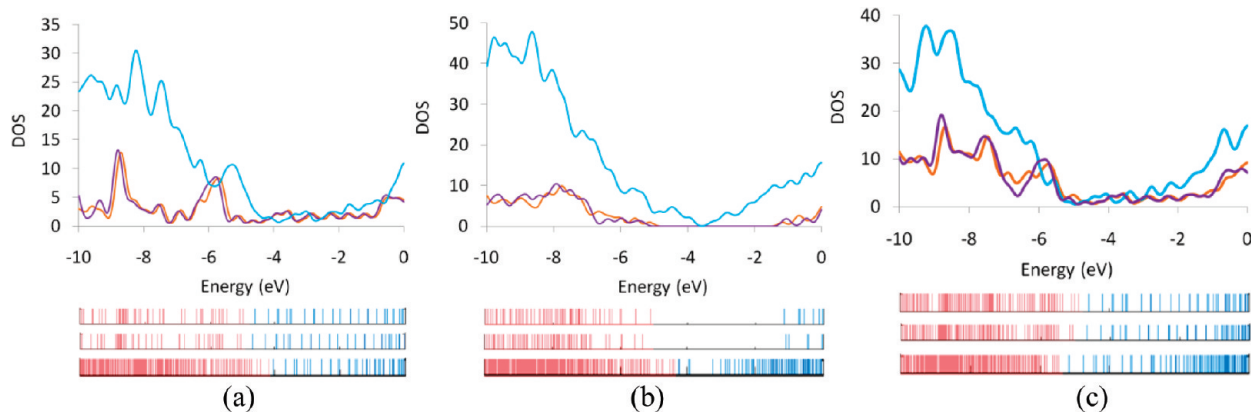


Figure 9. Density of states (DOS) spectrum for (a) carbon nanotube, (b) DNA, and (c) hybrid CNT–DNA structures using the DFT B3LYP/6-31G(d) level of theory. Top: curves for vacuum conditions (red), solvent conditions using PCM method (purple) and including water solvent molecules (cyan). Vertical lines at the bottom represent molecular orbital energies: red (occupied orbitals) and blue (unoccupied orbitals). The three sets of vertical lines correspond respectively, from top to down, to vacuum conditions, solvent conditions by using PCM method and solvent conditions by including water molecules.

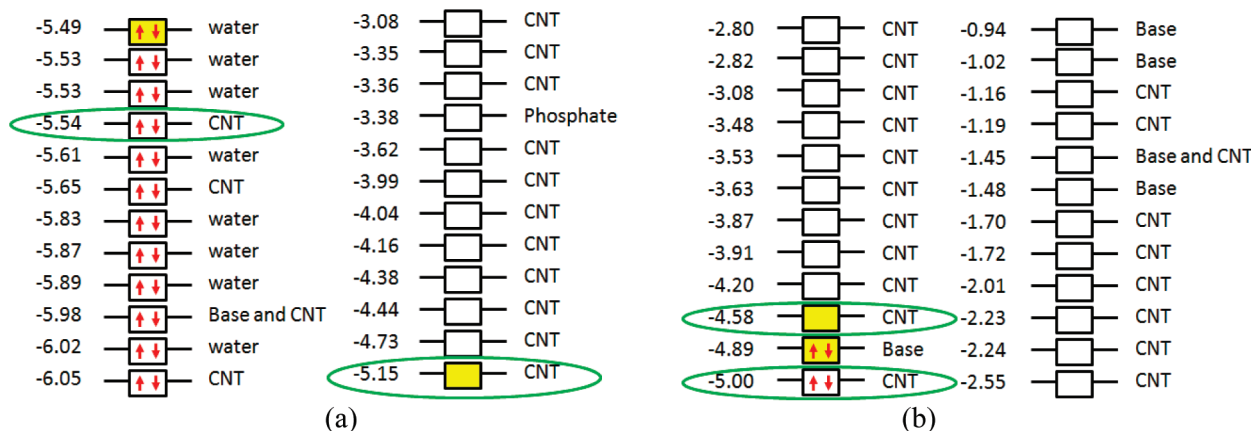


Figure 10. Molecular orbital energies (eV) for the CNT–DNA nanostructure in (a) water and (b) vacuum. Highlighted squares indicate HOMO and LUMO of the complex system. Green ellipses indicate carbon nanotube HOMO and LUMO. Orbitals are localized in the carbon nanotube (CNT), water molecules (water), bases (base), and phosphate groups (phosphate).

Table 3. HOMO, LUMO, and Gap Energies (eV) of DNA and CNT as Isolated Molecules and When They Are Part of the Complex DNA–CNT^a

system	Vacuum			PCM Solvent			Water Molecules			
	HOMO	LUMO	gap	HOMO	LUMO	gap	HOMO	LUMO	gap	
isolated	DNA	-5.14	-1.17	3.97	-5.37	-1.09	4.27	-5.93	-4.22	1.71
	CNT	-5.00	-4.59	0.41	-5.09	-4.66	0.43	-4.48	-4.04	0.44
complex	DNA	-4.89	-1.48	3.41	-5.50	-1.55	3.95	-5.98	-3.38	2.60
	CNT	-5.00	-4.58	0.43	-5.09	-4.66	0.43	-5.54	-5.15	0.39

^a Calculations are done in vacuum, under PCM solvent, and under actual water molecules in the Hamiltonian. All systems are run as uncharged and singlets.

on the DNA backbone; and also because a DNA molecule wrapped around the CNT breaks the symmetric electronic structure in the CNT–DNA hybrid system. The latter is because of the CNT highly polarizable electrons⁴³ since a polar electronic structure for the CNT–DNA hybrid make it more stable in water solvent conditions. Hardness of the complex decreases with water, making possible to absorb electromagnetic radiation at higher wavelengths.

Molecular orbital shapes corresponding to representative energy levels of CNT–DNA system are shown for water conditions and vacuum conditions in parts a–d of Figure 11. The molecular orbitals corresponding to lower energy levels above the LUMO orbital are mainly localized in CNT (Figure 10). In vacuum conditions, for energy levels above the LUMO, molecular orbitals are also localized in DNA bases. In water conditions, for energy levels above the LUMO, molecular

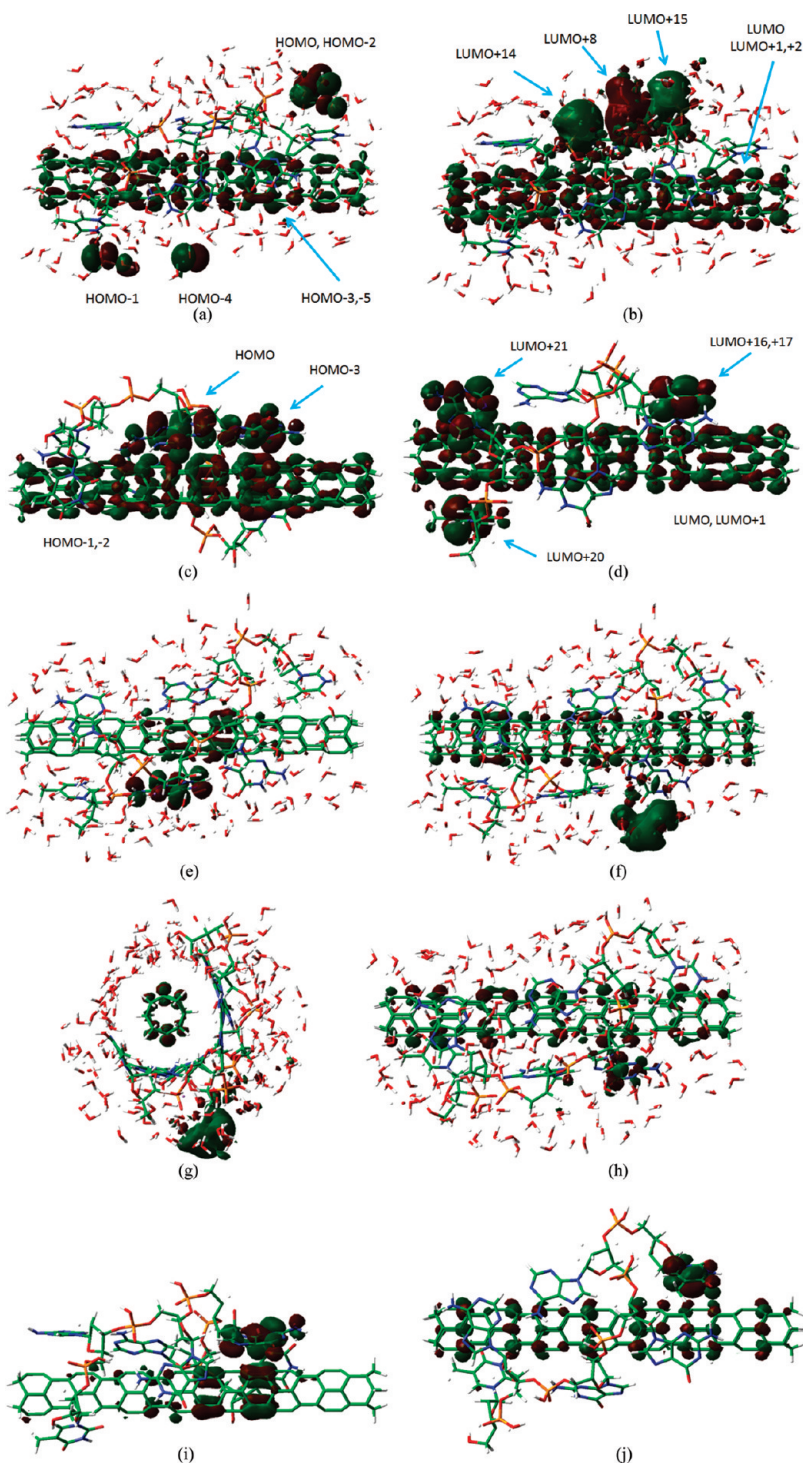


Figure 11. DNA sequence is (T1)(A1)(G1)(G2)(A2)(T2). Molecular orbital shapes for CNT–DNA system in water (a) HOMO (-5.49 eV) and HOMO-2 (-5.53 eV) are localized on the same region of water molecules. HOMO-3 (-5.54 eV) and HOMO-5 (-5.65 eV) are localized on CNT surface; (b) LUMO (-5.15 eV), LUMO+1 (-4.73 eV) and LUMO+2 (4.44 eV) are localized on CNT surface. LUMO+8 (-3.38 eV), LUMO+14 (-2.74 eV), and LUMO+15 (-2.72 eV) are localized in phosphate groups and its neighboring water molecules. LUMO+14 is localized between A1 and G1, LUMO+8 is localized between G1 and G2, LUMO+15 is localized between G2 and A2. Molecular orbital shapes for CNT–DNA system in vacuum (c) HOMO-1 (-5.0 eV) and HOMO-2 (-5.1 eV) are localized on CNT surface. HOMO (-4.89 eV) and HOMO-3 (-5.36 eV) are localized on G1 and G2, respectively; (d) LUMO and LUMO+1 are localized on CNT surface. LUMO+16 (-1.48 eV) and LUMO+17 (-1.45 eV) are both localized on T2 and CNT surface. LUMO+20 (-1.02 eV) and LUMO+21 (-0.94 eV) are localized on T1 and A1 respectively. Representative hybrid orbitals for CNT–DNA system in water (e) HOMO-9 (-5.98 eV) is localized on G1 and its neighboring CNT surface; (f), (g) LUMO+18 (-2.26 eV) and LUMO+19 (-2.25 eV) are both localized on water molecules and CNT surface. Water molecules are neighbors to G2; (h) LUMO+37 (-1.21 eV) is localized on G2 and CNT surface. Representative hybrid orbitals for CNT–DNA system in vacuum (i) HOMO-3 (-5.36 eV) is localized on G2 and its neighboring CNT surface; (j) LUMO+17 (-1.45 eV) is localized on T2 and CNT surface.

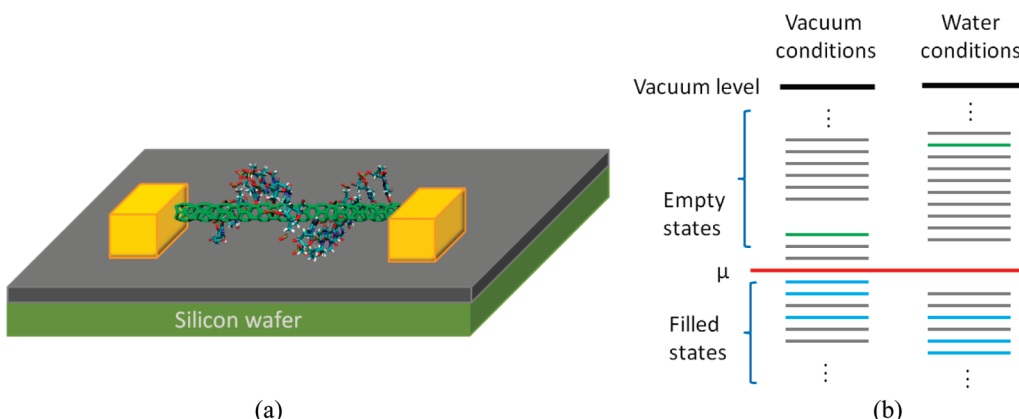


Figure 12. (a) Carbon nanotube–DNA based transistor and (b) its corresponding energy level diagram for vacuum conditions and water solvent conditions. Gray lines correspond to CNT energy states, green lines correspond to DNA molecule energy states, and cyan lines correspond to molecular orbitals shared by CNT and DNA. μ represents the gold electrode work function. Energy levels corresponding to water molecules are omitted for clarity.

orbitals are also localized on phosphate groups and DNA bases, with molecular orbitals corresponding to phosphate groups being mostly at lower energy levels than those corresponding to DNA bases. Molecular orbitals corresponding to phosphate groups are also localized in neighbor water molecules (part b of Figure 11).

We observe the presence of hybrid molecular orbitals, which allows a flow of electrons between carbon nanotube, DNA, and water molecules. Molecular orbital shapes are shown in parts e–j of Figure 11. Relative positions of energy levels for some hybrid orbitals are depicted in Figure 12. A DNA base is able to polarize the carbon nanotube electronic density in the region lying near to the DNA base as shown in parts e and i of Figure 11, breaking the nanotube electronic symmetry. The asymmetry, with respect to nanotube axial axis, of electronic density induced in carbon nanotube surface by the DNA base is higher in water conditions than in vacuum conditions. Molecular orbitals localized in DNA bases at relatively high energy levels, such as LUMO+17 and LUMO+37, are not able to produce an asymmetry in nanotube electronic density, as shown in parts g and j of Figure 11. Water molecules are able to produce a different kind of polarization as shown in parts f and g of Figure 11.

By constructing an energy level diagram (part b of Figure 12), and considering an approximate value of -5.3 eV for the gold electrode Fermi level, the DNA molecule yields a transistor-like gating mechanism as shown in Figure 12. Similar gating mechanism has been reported for a hybrid graphene–ssDNA system.⁷

Ouellette et al.³³ reported spikes in the time evolution of CNT electrical current as DNA molecules were allowed to flow through a microfluidic channel. Spikes current levels are below or above the original CNT current level depending on the type of DNA molecule tested. We suggest those spikes are produced every time a DNA molecule reaches the carbon nanotube surface, and a different change in current level, positive or negative spikes, is indicative of a DNA sequence dependent transistor-like gating mechanism. This DNA sequence dependence is further suggested by the known correlation between nucleobases polarizability and CNT–DNA interaction strength,³⁰ as well as the shift of HOMO and LUMO toward lower energy levels induced by DNA wrapping and reported in the present work. Changes in the electronic structure of CNT occur due to the breaking of electronic symmetry of CNT after DNA wrapping and to CNT having highly polarizable electrons, therefore, we expect a stronger DNA gating mechanism effect for single-walled carbon nanotubes with higher polarizability.

4. CONCLUSIONS

Ab initio electronic structure calculations have been performed for single-walled carbon nanotube, single-stranded DNA molecule, and DNA wrapped carbon nanotube considering in all cases vacuum conditions and water solvent conditions. Stable structural conformations in water solvent conditions are obtained from molecular dynamics simulations. In vacuum conditions, two factors contribute to a metallic behavior for CNT–DNA hybrid structure, mainly a decrease in DNA energy gap and the production of a hybrid structure energy gap smaller than in carbon nanotube. In water solvent conditions, an energy shift is produced in the HOMO and LUMO energy levels for the hybrid structure; we suggest this is due to the breaking of electronic symmetry in carbon nanotube produced by the wrapping of DNA molecule. Our results complement previous experimental and theoretical results on CNT–DNA interaction,^{30,32,33,43} providing further support for a DNA sequence dependent gating mechanism in suspended carbon nanotube (CNT) transistors, due to the key role played by CNT molecular polarizability on the breaking of electronic symmetry in the hybrid structure and to a correlation between nucleobases polarizability and CNT–DNA interaction strength. We hope to trigger further experiments needed to elucidate the specific DNA sequence dependence of this transistor-like gating mechanism in the carbon nanotube electrical characteristics.

■ AUTHOR INFORMATION

Corresponding Author

*To whom correspondence should be addressed: email seminario@tamu.edu.

■ ACKNOWLEDGMENT

This research was supported by a grant from U.S. Defense Threat Reduction Agency through the U.S. Army Research Office under grant number W911NF-06-1-0231.

■ REFERENCES

- (1) Tang, X.; Bansaruntip, S.; Nakayama, N.; Yenilmez, E.; Chang, Y.-I.; Wang, Q. Carbon nanotube DNA sensor and sensing mechanism. *Nano Lett.* **2006**, *6*, 1632–1636.
- (2) Pop, E.; Mann, D. A.; Goodson, K. E.; Dai, H. Electrical and thermal transport in metallic single-wall carbon nanotubes on insulating substrates. *J. Appl. Phys.* **2007**, *101*, 093710–10.

- (3) Chen, R. J.; Choi, H. C.; Bangsaruntip, S.; Yenilmez, E.; Tang, X.; Wang, Q.; Chang, Y.-L.; Dai, H. An investigation of the mechanisms of electronic sensing of protein adsorption on carbon nanotube devices. *J. Am. Chem. Soc.* **2004**, *126*, 1563–1568.
- (4) Derycke, V.; Martel, R.; Appenzeller, J.; Avouris, P. Controlling doping and carrier injection in carbon nanotube transistors. *Appl. Phys. Lett.* **2002**, *80*, 2773–2775.
- (5) Bellido, E. P.; Bobadilla, A. D.; Rangel, N. L.; Zhong, H.; Norton, M.; Sinitskii, A.; Seminario, J. M.; (2009) Current-voltage-temperature characteristics of DNA origami. *Nanotechnology* **20**
- (6) Guo, X.; Gorodetsky, A. A.; Hone, J.; Barton, J. K.; Nuckolls, C. Conductivity of a single DNA duplex bridging a carbon nanotube gap. *Nat Nano* **2008**, *3*, 163–167.
- (7) Lin, J. A.; Teweldebrhan, D.; Ashraf, K.; Liu, G. X.; Jing, X. Y.; Yan, Z.; Li, R.; Ozkan, M.; Lake, R. K.; Balandin, A. A.; Ozkan, C. S. Gating of single-layer graphene with single-stranded deoxyribonucleic acids. *Small* **2010**, *6*, 1150–1155.
- (8) Hong, S.; Jauregui, L. A.; Rangel, N. L.; Cao, H.; Day, S.; Norton, M. L.; Sinitskii, A. S.; Seminario, J. M. Impedance measurements on a DNA junction. *J. Chem. Phys.* **2008** *128*: 201103 (1–4)
- (9) Bobadilla, A. D.; Bellido, E. P.; Rangel, N. L.; Zhong, H.; Norton, M.; Sinitskii, A.; Seminario, J. M. DNA origami impedance measurement at room temperature. *J. Chem. Phys.* **2009** *130*.
- (10) Rangel, N. L.; Seminario, J. M. Vibronics and plasmonics based graphene sensors. *J. Chem. Phys.* **2010**, *132*, 125102.
- (11) Christancho, D.; Seminario, J. M.; (2010) Polypeptides in alpha-helix conformation perform as diodes. *J. Chem. Phys.* **132**: 065102 (1–5)
- (12) Rangel, N. L.; Sotelo, J. C.; , Seminario, J. M.; (2009) Mechanism of carbon-nanotubes unzipping into graphene ribbons. *J. Chem. Phys.* **131**: 031105:1–4
- (13) Rangel, N. L.; Seminario, J. M. Nano-micro interface to read molecular potentials into current-voltage based electronics. *J. Chem. Phys.* **2008**, *128*, 114711.
- (14) Seminario, J. M.; Araujo, R. A.; Yan, L. Negative Differential Resistance in Metallic and Semiconducting Clusters. *J. Phys. Chem. B* **2004**, *108*, 6915–6918.
- (15) Derosa, P. A.; Guda, S.; Seminario, J. M. A programmable molecular diode driven by charge-induced conformational changes *J. Am. Chem. Soc.* **2003**, *125*, 14240–14241.
- (16) Seminario, J. M.; De La Cruz, C.; Derosa, P. A.; Yan, L. Nanometer-size conducting and insulating molecular devices. *J. Phys. Chem. B* **2004**, *108*, 17879–17885.
- (17) Staici, C.; Johnson, A. T.; Chen, M.; Gelperin, A. DNA-decorated carbon nanotubes for chemical sensing. *Nano Lett.* **2005**, *5*, 1774–1778.
- (18) Chen, C. L.; Yang, C. F.; Agarwal, V.; Kim, T.; Sonkusale, S.; Busnaina, A.; Chen, M.; , Dokmeci, M. R. DNA-decorated carbon-nanotube-based chemical sensors on complementary metal oxide semiconductor circuitry. *Nanotechnology* **2010** *21*.
- (19) Lu, G.; Maragakis, P.; Kaxiras, E. Carbon nanotube interaction with DNA. *Nano Lett.* **2005**, *5*, 897–900.
- (20) Meng, S.; Kaxiras, E., “Interaction of DNA with CNTs: Properties and Prospects for Electronic Sequencing,” in *Biosensing Using Nanomaterials*; Merkoci, A., Ed., 1st ed: Wiley-Interscience: New York, 2009; pp 67–96.
- (21) Rangel, N. L.; Seminario, J. M. Single molecule detection using graphene molecules. *J. Phys. B* **2010**, *43*, 155101.
- (22) Wang, K.; Rangel, N. L.; Kundu, S.; Sotelo, J. C.; Tovar, R. M.; Seminario, J. M.; Liang, H. Switchable molecular conductivity. *J. Am. Chem. Soc.* **2009**, *131*, 10447–10451.
- (23) Rangel, N. L.; Williams, K. S.; Seminario, J. M. Light-activated molecular conductivity in the photoreactions of vitamin D₃. *J. Phys. Chem. A* **2009**, *113*, 6740–6744.
- (24) Jauregui, L. A.; Salazar-Salinas, K.; Seminario, J. M. Transverse electronic transport in double-stranded DNA nucleotides. *J. Phys. Chem. B* **2009**, *113*, 6230–6239.
- (25) Gimenez, A. J.; Luna-Bárcenas, G.; Seminario, J. M. Emulation of molecular programmability using microelectronic programmable devices. *J. Phys. Chem. C* **2009**, *36*, 16254–16258.
- (26) Gimenez, A. J.; G. Luna-Barcenas, Seminario, J. M. Analysis of nano and molecular arrays of negative differential resistance devices for sensing and electronics. *IEEE Sensors* **2009** *9*: No 9.
- (27) Rangel, N. L.; Seminario, J. M. Graphene terahertz generators for molecular circuits and sensors. *J. Phys. Chem. A* **2008**, *112*, 13699–13705.
- (28) Juarregui, L. A.; Seminario, J. M. A DNA sensor for sequencing and mismatches based on electron transport through Watson–Crick and non-Watson–Crick base pairs. *IEEE Sensors* **2008**, *8*, 803–814.
- (29) Gowtham, S.; Scheicher, R. H.; Ahuja, R.; Pandey, R.; Karna, S. P. Physisorption of nucleobases on graphene: Density-functional calculations. *Phys. Rev. B* **2007**, *76*, 033401.
- (30) Gowtham, S.; Scheicher, R. H.; Pandey, R.; Karna, S. P.; Ahuja, R. First-principles study of physisorption of nucleic acid bases on small-diameter carbon nanotubes. *Nanotechnology* **2008**, *19*, 125701.
- (31) Johnson, R. R.; Johnson, A. T. C.; Klein, M. L. Probing the structure of DNA–Carbon nanotube hybrids with molecular dynamics. *Nano Lett.* **2007**, *8*, 69–75.
- (32) Cha, M.; Jung, S.; Cha, M.-H.; Kim, G.; Ihm, J.; Lee, J. Reversible metal–semiconductor transition of ssDNA-decorated single-walled carbon nanotubes. *Nano Lett.* **2009**, *9*, 1345–1349.
- (33) Ouellette, L. Chemical and biological sensing with carbon nanotube in solution. PhD Thesis, Cornell University, Ithaca, NY, 2008.
- (34) Plimpton, S. Fast parallel algorithms for short-range molecular dynamics. *J. Comput. Phys.* **1995**, *117*, 1–19.
- (35) Jorgensen, W. L.; Chandrasekhar, J.; Madura, J. D.; Impey, R. W.; Klein, M. L. Comparison of simple potential functions for simulating liquid water. *J. Chem. Phys.* **1983**, *79*, 926–935.
- (36) MacKerell, A. D.; Bashford, D.; Bellott, R. L.; Dunbrack, J. D.; Evanseck, M. J.; Field, S.; Fischer, J.; Gao, H.; Guo, S.; Ha, D.; Joseph-McCarthy, L.; Kuchnir, K.; Kuczera, F. T. K.; Lau, C.; Mattos, S.; Michnick, T.; Ngo, D. T.; Nguyen, B.; Prodhom, W. E.; Reiher, B.; Roux, M.; Schlenkrich, J. C.; Smith, R.; Stote, J.; Straub, M.; Watanabe, J.; Wiorkiewicz-Kuczera, D.; Yin, Y.; Karplus, M. All-atom empirical potential for molecular modeling and dynamics studies of proteins. *J. Phys. Chem. B* **1998**, *102*, 3586–3616.
- (37) Martínez, L.; Andrade, R.; Birgin, E. G.; Martínez, J. M. *Packmol*: A package for building initial configurations for molecular dynamics simulations. *J. Comput. Chem.* **2009**, *30*, 2157–2164.
- (38) Hockney, R. W.; Eastwood, J. W. *Computer Simulation Using Particles*; Taylor & Francis, Inc., 1988.
- (39) Berendsen, H. J. C.; Postma, J. P. M.; Vangunsteren, W. F.; Dinola, A.; Haak, J. R. Molecular dynamics with coupling to an external bath. *J. Chem. Phys.* **1984**, *81*, 3684–3690.
- (40) Humphrey, W.; Dalke, A.; Schulter, K. VMD: Visual molecular dynamics. *J. Mol. Graphics* **1996**, *14*, 33–38.
- (41) Brooks, B. R.; Bruccoleri, R. E.; Olafson, B. D.; States, D. J.; Swaminathan, S.; Karplus, M. CHARMM: A program for macromolecular energy, minimization, and dynamics calculations. *J. Comput. Chem.* **1983**, *4*, 187–217.
- (42) Miertus, S.; Scrocco, E.; Tomasi, J. Electrostatic interaction of a solute with a continuum. A direct utilization of AB initio molecular potentials for the revision of solvent effects. *Chem. Phys.* **1981**, *55*, 117–129.
- (43) Rotkin, S. V. Electronic properties of nonideal nanotube materials: Helical symmetry breaking in DNA hybrids. In *Annual Review of Physical Chemistry*, vol. 61; Palo Alto: Annual Reviews, **2010**, pp 241–261.